Korean J. Chem. Eng., 36(6), 975-980 (2019)
DOI: 10.1007/s11814-018-0231-0

pISSN: 0256-1115
eISSN: 1975-7220

Surface-enhanced infrared detection of benzene in air using a porous metal-organic-frameworks film

Raekyung Kim*,‡, Seohyeon Jee*,‡, Unjin Ryu*, Hyeon Shin Lee*, Se Yun Kim,†, and Kyung Min Choi*,†**

*Department of Chemical and Biological Engineering, Sookmyung Women's University, 100 Cheongpa-ro 47 gil, Yongsan-gu, Seoul 04310, Korea
**Department of Materials Science & Engineering, KAIST, Daejeon 34141, Korea
(*Received 31 October 2018 • accepted 17 January 2019*)

Abstract–Infrared (IR) spectroscopy is a powerful technique for observing organic molecules, as it combines sensitive vibrational excitations with a non-destructive probe. However, gaseous volatile compounds in the air are challenging to detect, as they are not easy to immobilize in a sensing device and give enough signal by themselves. In this study, we fabricated a thin nanocrystalline metal-organic framework (nMOF) film on a surface plasmon resonance (SPR) substrate to enhance the IR vibration signal of the gaseous volatile compounds captured within the nMOF pores. Specifically, we synthesized nanocrystalline HKUST-1 (nHKUST-1) particles of *ca.* 80 nm diameter and used a colloidal dispersion of these particles to fabricate nHKUST-1 films by a spin-coating process. After finding that benzene was readily adsorbed onto nHKUST-1, an nHKUST-1 film deposited on a plasmonic Au substrate was successfully applied to the IR detection of gaseous benzene in air using surface-enhanced IR spectroscopy.

Keywords: Metal-organic Frameworks, Porous Film, Surface-enhanced IR Spectroscopy, Volatile Organic Compounds, Plasmon Resonance

INTRODUCTION

Surface-enhanced infrared (IR) absorption spectroscopy (SEIRAS), which exploits the signal enhancement induced by the surface plasmon resonance (SPR) of thin metal films [1-3], has proven to be a powerful method to improve the IR detection limits of molecules whose small absorption cross sections do not provide adequate IR signal. Such enhanced IR absorption has been utilized in various sensor, photonics, and enhanced spectroscopy applications [4-16]. However, these applications are generally limited to molecules immobilized on the plasmonic surface, as the plasmon enhancement decays exponentially with distance. For gaseous organic molecules in air, their surface-enhanced IR detection has been challenging, as they are not easily immobilized on the plasmonic surface and usually co-exist with other gases in air. Especially for the non-polar volatile organic compounds (VOCs) such as benzene, they are necessarily required to be concentrated from the air on either an adsorbent or by trapping whole air in a container, followed by using gas chromatography (GC) [17], Fourier transform infrared spectrometer (FT-IR) [18], proton transfer reaction mass spectrometer (PTR-MS) [19], and membrane interface mass spectrometry [20]. Therefore, these processes all need large amount of air and long process time for measuring benzene in air.

A metal-organic framework (MOF) is known as a functional microporous material capable of capturing target molecules existing in air. We envisioned that a thin layer of an MOFs coated on a plasmonic metal film can capture target gases sufficiently near the plasmonic surface to enhance their IR signal (Fig. 1). In this report, we prepared colloidal solutions of nanocrystalline MOFs (nMOFs) and fabricated an nMOF layer on a SPR film to test the surface-enhanced IR detection of benzene. Specifically, we chose HKUST-1 as an exemplar case of MOF, as it is known to have high sorption capability of benzene even in low partial pressure region [21-25]. The HKUST-1 was synthesized in nanocrystalline form (*ca.* 80 nm, referred to as nHKUST-1) with a homogeneous particle size and morphological distribution at room temperature. The nHKUST-1 particles were dispersed in hexane containing oleic acid as a surface modulator to give a colloidal solution, which was then used in a spin-coating process to fabricate an nHKUST-1 layer on an Au

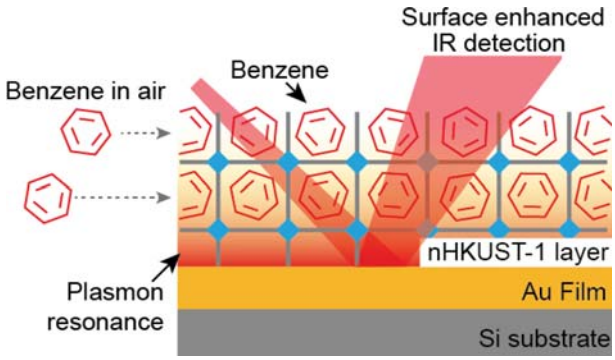

Fig. 1. Schematic diagram for surface-enhanced IR detection of benzene in air using an nHKUST-1 layer fabricated on the Au substrate.

†To whom correspondence should be addressed.
E-mail: ksyvip@kaist.ac.kr, kmchoi@sookmyung.ac.kr
‡These authors contributed equally.

thin film [26]. After confirming that the nHKUST-1 particles showed high sorption of benzene, the nHKUST-1 film coated on the Au substrate was successfully used to provide the clear vibrational intensity of benzene in air while other films without having either the nHKUST-1 film and the Au substrate were not. This is the report regarding the fabrication of an nMOF layer on a plasmonic substrate by spin-coating process to achieve the surface-enhanced IR detection of benzene in air.

The synthesis of nMOFs was combined with plasmon enhancement in various application fields, including surface-enhanced Raman scattering (SERS) [27-29], SEIRA [30,31], and photosynthesis [10, 32,33] (Table S1). Recently, plasmon enhanced MOF films for on-chip gas sensing have been reported [4], but surface-enhanced IR detection using a nanocrystalline MOF film is still challenging. Previous studies using other materials for the detection of gaseous molecules using spectroscopy have mainly focused on using ultraviolet-visible region [11-14,16,34-37] (Table S2), and the enhanced IR detection still remains challenging. In an attempt to overcome these challenges, we developed an nMOF-based spin-coating process to produce a porous film on SPR substrate and then achieved the surface-enhanced IR detection of gaseous organic compounds.

MATERIAL AND METHODS

1. Chemicals

All reagents were obtained from commercial sources unless otherwise stated and used without further purification. 1,3,5-Benzenetricarboxylic acid (H_3BTC, 95%), trimethylamine (≥99%), *N,N*-dimethylformamide (DMF, ≥99%), and copper(II) acetate monohydrate ($Cu(OAc)_2 \cdot H_2O$, ≥98%) were purchased from Sigma-Aldrich. Ethanol, acetone, and distilled water were purchased from Duksan. Hexane (95%) was purchased from Samchun. Hypophosphorous acid (50 wt% solution in water) was purchased from Acros.

2. Synthesis of nHKUST-1

nHKUST-1 was synthesized using a previously reported process with slight modifications [24]. First, 215 mg of $Cu(OAc)_2 \cdot H_2O$ was dissolved in 5 mL of DMF in a 20 mL vial, and 126 mg of H_3BTC and 0.25 mL of triethylamine were dissolved in 2 mL of DMF in a separate vial. These two solutions were then combined into a single solution in a mixture of DMF (18 mL), ethanol (25 mL), and water (25 mL) in a round flask. The mixture was vigorously stirred with a magnetic stir bar for 1 h at room temperature. The resulting nHKUST-1 was washed twice with DMF using a centrifuge (7,000 rpm for 10 min) and sonication. The nHKUST-1 was then sequentially immersed in acetone for a 24 h period three times. Finally, the nHKUST-1 was activated by removing the solvent under vacuum for about 5 h. The final product was obtained as a blue powder.

3. nHKUST-1 Film Fabrication Process

70 mg of nHKUST-1 was introduced into a hexane solution containing 53 μL of oleic acid and dispersed using sonication for 3 h. In the meantime, the substrates were soaked in hypophosphorous acid (50 wt% solution in water) and sonicated for 1 h to clean their surfaces, and then washed with ethanol, acetone, and water for 1 h each. The substrates were dried using a N_2 stream, and then the nHKUST-1 colloidal solution was deposited and spin-coated on the substrates (7,000 rpm, 2 min). The oleic acid remaining in the nHKUST-1 film was washed out by soaking the coated substrates in acetone followed by drying with a N_2 stream.

4. Surface-enhanced IR Detection

The Si substrate was placed on the top of a thermal evaporator (thermal evaporator system KVT-D665) and then Au source was deposited on the Si substrate for 5 min to produce an Au/Si substrate in a thickness of ~250 nm (Fig. S1). The planar SEM image for the Au/Si substrate revealed that the Au layer is composed of nanoparticles (~50 nm in diameter) and have rugged surface (Fig. S1). This surface morphology is advantageous to make the nHKUST-1 particles deposited well on its surface during the spin-coating process, as well as making the plasmonic effect strong for the surface-enhanced IR detection of benzene [38,39]. An nHKUST-1 film was deposited on the surface (nHKUST-1/Au/Si) using the same procedure described above using 2.4 wt% nHKUST-1 colloidal dispersion. For the sorption of benzene within the pores of nHKUST-1 film, the nHKUST-1/Au/Si sample was placed in a sealed chamber containing 1 ml of benzene inside for an hour in room temperature, which makes 12.67 vol% of benzene in air. The excess benzene existing outside of pores in nHKUST-1 was removed by drying the sample in ambient condition. The nHKUST-1/Au/Si sample having benzene molecules inside of its pore was then transferred into an FT-IR spectrometer (Nicolet IS50) for ATR diamond mode measurement. The IR scan range was 1,000-1,200 nm with 32 scans for 2 min. Controlled samples of the nHKUST-1 particles (nHKUST-1), an nHKUST-1 film on a Si substrate (nHKUST-1/Si), and an nHKUST-1 film on an Au-coated Si substrate (nHKUST-1/Au/Si) were all tested in the same procedure.

5. Characterization

The powder X-ray diffraction (PXRD) spectra were obtained using a Rigaku X-ray diffractometer (Smartlab, Cu Kα radiation) at 1,200 W (40 kV, 30 mA) at a scan rate of 4°/min from 3° to 50° on a silicon holder. Field emission scanning electron microscopy (FE-SEM) was carried out at 3 kV using a JEOL JSM-7600F microscope. For SEM observation, the nHKUST-1 particles were dispersed in acetone and placed on a silicon substrate. Pt was coated onto the samples before they were placed in the SEM chamber. The SEM observations were carried out in GB_LOW mode, with a WD of 8.0 mm. The nHKUST-1 film was observed in the same way. Solvent and gas adsorption analysis was performed using a BELSORP-max automatic and volumetric adsorption analyzer. Before the gas and solvent sorption measurements, the samples were activated at 150 °C for 24 h followed by a purge with nitrogen.

RESULTS AND DISCUSSION

1. Synthesis and Characterization of nHKUST-1 Particles

Nanocrystalline HKUST-1 particles were synthesized by inducing massive nucleation at room temperature. A burst of nHKUST-1 nucleation was triggered by adding triethylamine to a solution of $Cu(OAc)_2 \cdot H_2O$ and 1,3,5-benzenetricarboxylic acid in a 1 : 1 : 1 mixture of DMF/EtOH/H_2O at room temperature, which resulted in the formation of nanocrystalline particles at room temperature. After 1 h of reaction, the resulting particles were washed with DMF to remove unreacted chemicals and then with acetone to exchange

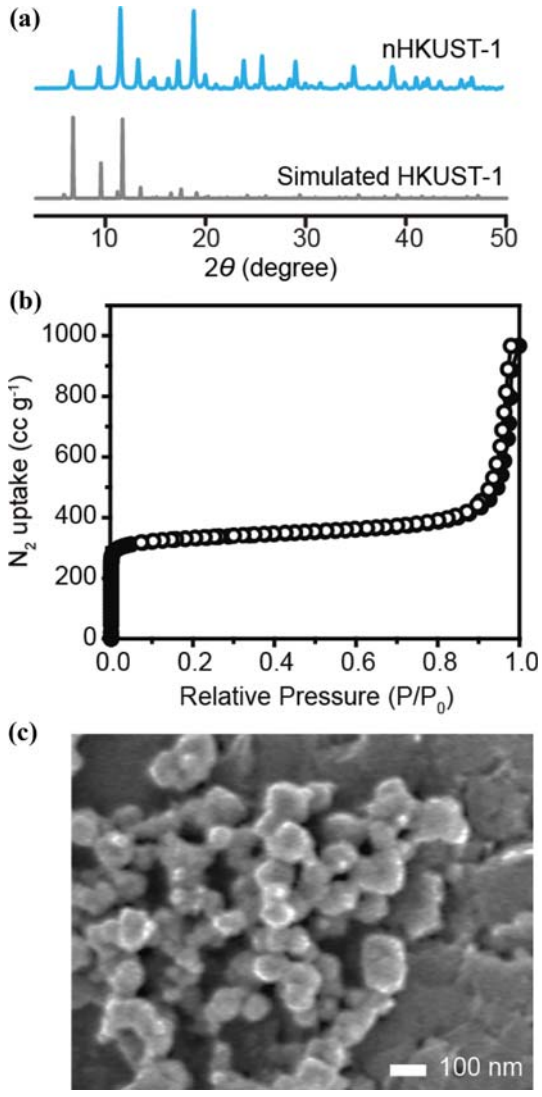

Fig. 2. (a) X-ray diffraction pattern of nHKUST-1 and the simulated pattern of HKUST-1. (b) N_2 adsorption isotherms for nHKUST-1 at 77 K with adsorption and desorption points represented by solid and open circles, respectively. (c) SEM image of nHKUST-1.

the DMF, followed by drying in a vacuum oven.

The crystallinity of nHKUST-1 was confirmed by PXRD analysis (Fig. 2(a)). The experimental diffraction patterns of nHKUST-1 matched the diffraction patterns simulated for HKUST-1, indicating that the crystal structure of nHKUST-1 was identical to that of the single crystals of HKUST-1 [40]. Infrared (IR) and Raman spectroscopy also indicated the chemical natures are identical, even in nanocrystalline form (Fig. S2 and S3) [22,41]. The permanent porosity of nHKUST-1 was also confirmed by the measurement of its nitrogen adsorption isotherm, which showed type-I sorption behavior expected for this MOF (Fig. 2(b)). The Langmuir surface area of the nanocrystalline HKUST-1 was 1,370 m^2/g, which was within the range of bulk HKUST-1 (917.6-2,175 m^2/g) [42]. A representative scanning electron microscopy (SEM) (Fig. 2(c)) and transmission electron microscopy (TEM) (Fig. S4) images of nHKUST-1 shows that the nHKUST-1 particles were approximately *ca.* 80 nm in diameter, uniform in size, and demonstrated identical spherical geometry.

2. Dispersion of nHKUST-1 Particles

As we intended to use a spin-coating process for fast and controllable formation of the nHKUST-1 film, the nHKUST-1 particles had to be dispersed in a volatile solvent. However, the surface of nHKUST-1 has many dangling bonds and incompletely bonded metal oxide, which makes nHKUST-1 particles hydrophilic. Our strategy to produce a well dispersed colloidal solution was to use oleic acid as a surfactant, and then disperse the oleic acid coated nHKUST-1 in a non-polar solvent. Oleic acid has a terminal carboxylic group that bonds with the surface of nHKUST-1, and hydrocarbon chains that interact strongly with non-polar solvents such as hexane. The addition of nHKUST-1 particles directly to hexane would result in the formation of large aggregates because the hydrophilic surface of nHKUST-1 interacts unfavorably with the non-polar solvent hexane. However, when nHKUST-1 was added to a mixture of hexane and oleic acid and subjected to sonication for 3 h, a colloidal dispersion of nHKUST-1 was successfully formed (Fig. 3(a)). The colloidal solution maintained its dispersion and was used for the thin-film fabrication the next step.

3. Fabrication and Control of nHKUST-1 Film

The formation of nHKUST-1 films was tested on glass substrates that had been pretreated with hypophosphorous acid (50 wt% solution in water) for 1 h followed by washing with acetone, ethanol, and water. Fully dispersed colloidal solutions containing 1.0 wt%, 2.4 wt%, or 5 wt% of nHKUST-1 in hexane were spread onto the cleaned substrates and assembled into thin films by spin-coating (7,000 rpm, 2 min). The surface morphology and thickness of the nHKUST-1 films were observed using SEM and atomic force microscopy (AFM), and the crystallinity of the films was examined by PXRD analysis. As shown in Fig. 3(b), translucent blue nHKUST-1 thin films were successfully fabricated on a large-area transparent substrate.

The films were uniformly deposited over the entire surface of the substrate for all the tested concentrations of nHKUST-1, as shown in the planar SEM images in Fig. 3(c)-(e) and the AFM image in Fig. S5. The thickness of the films depended on the concentration of the colloidal solution; concentrations of 1.0 wt%, 2.4 wt%, and 5 wt% formed 80-nm, 400-nm, and 1,000-nm thick nHKUST-1 films, respectively (Fig. 3(f)-(h)). Note that the 80-nm-thick film consisted of a single layer of nHKUST-1 particles, as shown in Fig. 3(f). As SPR decays exponentially with the distance to the substrate, a single layer of nHKUST-1 was considered to be most suitable to achieve surface-enhanced IR detection. The crystallinity of each of the nHKUST-1 films was evident from their PXRD diffraction lines (Fig. S6), and the preservation of the crystal structure was demonstrated by the coincidence of the diffraction lines for the films with those of the nHKUST-1 particles. We also tested the formation of nHKUST-1 films on glass, silicon and Ti-metal substrates (Fig. 3(i)-(k)). A thin film was successfully formed on all of the tested substrates, and all of the films showed a similar thickness of *ca.* 100 nm. This confirmed that our spin coating process could be applied to plasmonic substrates to achieve specific functions and interactions with guest molecules trapped in the porous MOF films.

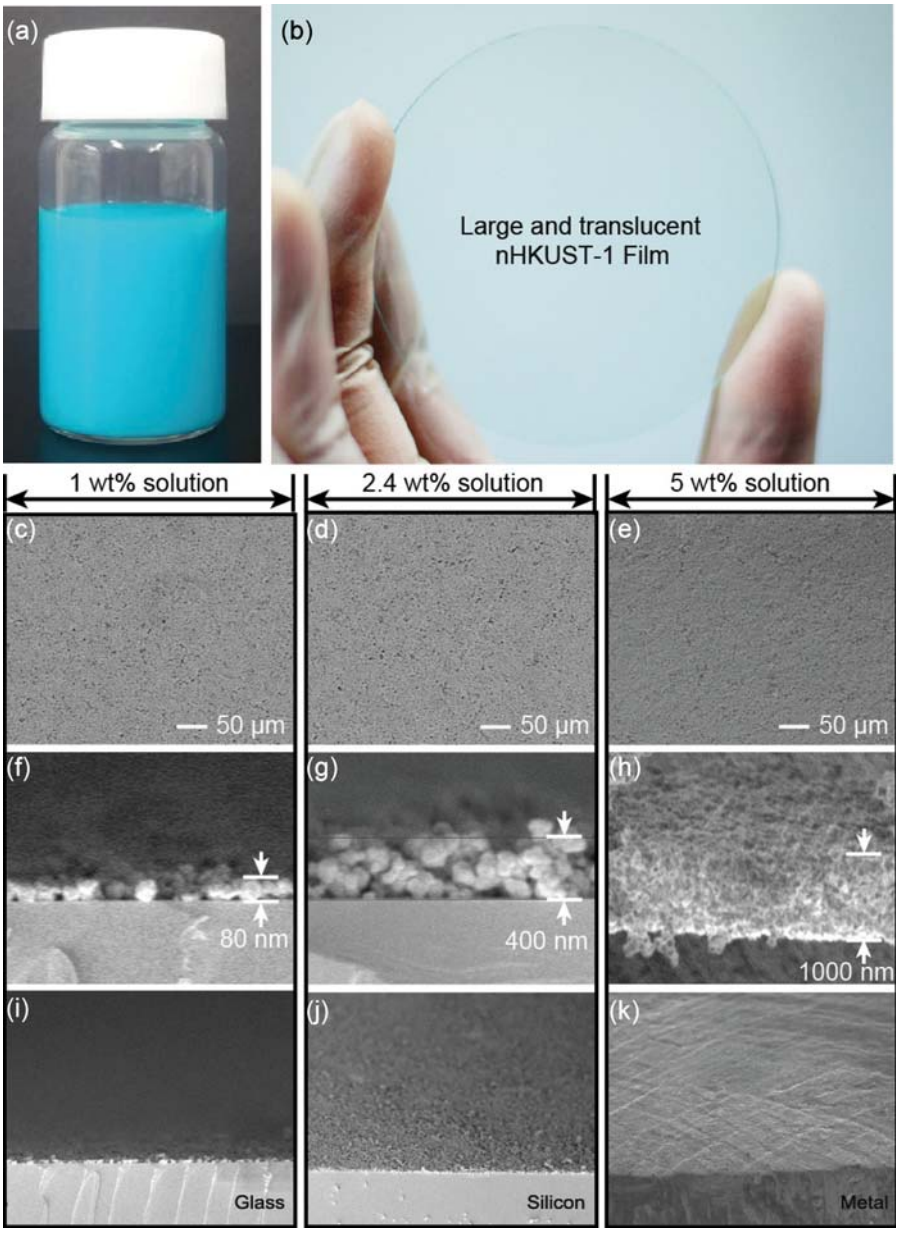

Fig. 3. (a) Photograph of the nHKUST-1 colloidal dispersion. (b) Translucent blue nHKUST-1 thin film on a large-area transparent substrate. (c)-(e) Planar and (f)-(h) cross-sectional SEM images of the nHKUST-1 films fabricated using nHKUST-1 colloidal solutions with different concentrations of (c), (f) 1 wt% solution; (d), (g) 2.4 wt% solution; (e), (h) 5 wt% solution. (i)-(k) nHKUST-1 films deposited on different substrates.

4. Benzene Sorption in nHKUST-1

The surface-enhanced IR performance of the nHKUST-1 film for the detection of molecules in the air was tested using benzene as the target molecule. The sorption capacity of nHKUST-1 for benzene at room temperature was first tested to determine whether the nHKUST-1 particles could trap benzene molecules inside. The sorption capacity was measured by evaporating liquid benzene at room temperature using a Belsorp-Max, and the results are presented in Fig. 4(a). The benzene sorption isotherm showed a type-I sorption behavior, indicating that benzene is rapidly adsorbed in the very low-pressure region and get saturated when relative pressure reaches about 0.08. This data was in good agreement with a previous report [21,22,40]. It is believed that the micropores of nHKUST-1, which are composed of a number of benzene rings, have a hydrophobic character and thus enhance the sorption capacity towards hydrophobic benzene in the low-pressure region. Considering the low sorption capability of nitrogen, carbon dioxide, and toluene in room temperature (Fig. S7), benzene is favorable to be captured within nHKUST-1 film, where their proximity to the SPR-active plasmonic substrate should result in the enhanced IR detection of benzene.

5. Surface-enhanced Infrared Detection of Benzene in Air Using an nHKUST-1 Film

To evaluate the SPR-enhanced detection of benzene on various

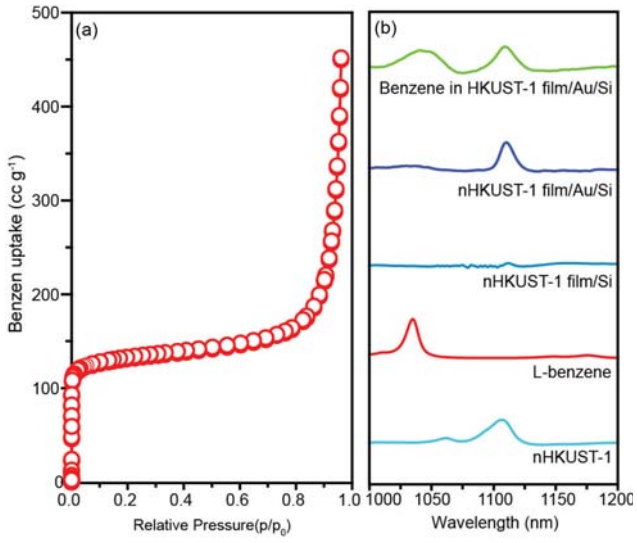

Fig. 4. (a) The sorption isotherm of benzene in nHKUST-1 at room temperature. (b) FT-IR spectra for nHKUST-1 particles (nHKUST-1), liquid benzene (L-benzene), an nHKUST-1 film on a Si substrate (nHKUST-1/Si), an nHKUST-1 film on a Au-coated Si substrate (nHKUST-1/Au/Si), and an nHKUST-1 film with adsorbed benzene on a Au-coated Si substrate (Benzene/nHKUST-1/Au/Si).

nHKUST-1 coated substrates, the attenuated total reflectance (ATR) FT-IR spectra of the nHKUST-1 particles (nHKUST-1), liquid benzene (L-benzene), an nHKUST-1 film on a Si substrate (nHKUST-1/Si), an nHKUST-1 film on Au-coated Si substrate (nHKUST-1/Au/Si), and an nHKUST-1 film with adsorbed benzene on Au-coated Si substrate (benzene/nHKUST-1/Au/Si) samples were measured using a Nicolet IS50 from Thermo Scientific ATR-FT-IR Spectrometer (Fig. 4(b)). To prepare the benzene/nHKUST-1/Au/Si sample, benzene was adsorbed onto the nHKUST-1 film through the evaporation of L-benzene in a sealed chamber at room temperature. The characteristic vibrations of the nHKUST-1 and L-benzene samples were observed at 1,120 and 1,043 cm^{-1}, respectively, which agreed with previous reports [5,22]. For the nHKUST-1 film fabricated on a Si substrate, the signal at 1,120 cm^{-1} was present, but was difficult to distinguish from the background. For the nHKUST-1 film on the Au substrate, the signal corresponding to nHKUST-1 was enhanced more than three-fold compared with that observed for the Si substrate. This was attributed to the surface-enhanced IR absorption of the nHKUST-1 film as a result of being sufficiently close to the SPR produced by the Au substrate. The IR spectrum of the benzene/nHKUST-1/Au/Si sample shows strongly enhanced vibration signals at 1,120 and 1,043 cm^{-1} for nHKUST-1 and benzene, respectively. The sensitivity for benzene is about 6.3×10^{-3} area/vol% at vibration signal of 1,043 cm^{-1}. It is noteworthy that the samples without either nHKUST-1 or Au layer on Si substrate did not show any vibrational signal for benzene, even when extended exposure and measurement times were used. These results indicate that our method of fabricating a porous thin film of a MOF on a plasmonic substrate provides a facile way to observe gas molecules using surface-enhanced IR detection, and provides the possibility to further investigate their gas-state reaction mechanisms using enhanced *in-situ* IR signals.

CONCLUSIONS

We have demonstrated a fast and controllable way to achieve surface-enhanced IR detection of benzene by fabricating porous nHKUST-1 films on a plasmonic substrate using a spin coating process. We synthesized homogeneously distributed nHKUST-1 particles with a diameter of *ca.* 80 nm and dispersed them in a volatile solvent to form a colloidal dispersion. The solution was deposited on various substrates, and thin films were formed using a spin coating process. The nHKUST-1 films were then coated onto Au-coated substrates capable of producing SPR. The vibration signals of the benzene captured within the pores of the nHKUST-1 film were greatly enhanced by the plasmon resonance, allowing the detection of benzene in air. The fast and controllable formation of the microporous MOF film on the plasmonic substrate provides a synergistic combination for the surface-enhanced IR detection of volatile organic compounds.

ACKNOWLEDGEMENTS

This research was supported by the Basic Science Research Programs of the National Research Foundation of Korea (NRF) (2016R1C1B1010781 and 2017K2A9A1A06060915), and partially by Sookmyung Women's University Research Grant (1-1703-2035).

SUPPORTING INFORMATION

Additional information as noted in the text. This information is available via the Internet at http://www.springer.com/chemistry/journal/11814.

REFERENCES

1. A. Hartstein, J. R. Kirtley and J. C. Tsang, *Phys. Rev. Lett.*, **45**, 201 (1980).
2. A. Hatta, T. Ohshima and W. Suetaka, *Appl. Phys. A.*, **29**, 71 (1982).
3. F. Neubrech, C. Huck, K. Weber, A. Pucci and H. Giessen, *Chem. Rev.*, **117**, 5110 (2017).
4. X. Chong, Y. Zhang, E. Li, K. Kim, P. R. Ohodnicki, C. Chang and A. X. Wang, *ACS Sens.*, **3**, 230 (2018).
5. B. C. Smith, *Spectroscopy*, **31**, 34 (2016).
6. M. Osawa, *Top. Appl. Phys.*, **81**, 163 (2001).
7. J. Kundu, F. Le, P. Nordlander and N. J. Halas, *Chem. Phys. Lett.*, **452**, 115 (2008).
8. A. Yamakata, T. Uchida, J. Kubota and M. Osawa, *J. Phys. Chem. B*, **110**, 6423 (2006).
9. A. Miki, S. Yeb and M. Osawa, *Chem. Commun.*, **14**, 1500 (2002).
10. L. E. Kreno, J. T. Hupp and R. P. V. Duyne, *Anal. Chem.*, **82**, 8042 (2010).
11. N. A. Joy, M. I. Nandasiri, P. H. Rogers, W. Jiang, T. Varga, S. V. N. T. Kuchibhatla, S. Thevuthasan and M. A. Carpenter, *Anal. Chem.*, **84**, 5025 (2012).
12. E. D. Gaspera and A. Martucci, *Sensors*, **15**, 16910 (2015).
13. E. D. Gaspera, A. Mura, E. Menin, M. Guglielmi and A. Martucci,

Sens. Actuators, B, **187**, 363 (2013).
14. N. A. Karker, G. Dharmalingam and M. A. Carpenter, *Nanoscale*, **7**, 17798 (2015).
15. S. Bai, H. Liu, J. Sun, Y. Tian, R. Luo, D. Li and A. Chena, *RSC Adv.*, **5**, 48619 (2015).
16. H. C. Kim, C. S. Park, K. M. Kang, M. H. Hong, Y. J. Choi and H. H. Park, *New J. Chem.*, **39**, 2256 (2015).
17. C. P. Weisel, *Chem. Biol. Interact.*, **184**, 58 (2010).
18. J. D. Jeffers, C. B. Roller and K. Namjou, *Anal. Chem.*, **76**, 424 (2004).
19. E. Velasco1, B. Lamb, H. Westberg, E. Allwine, G. Sosa, J. L. Arriaga-Colina, B. T. Jobson, M. L. Alexander, P. Prazeller, W. B. Knighton, T. M. Rogers, M. Grutter, S. C. Herndon, C. E. Kolb, M. Zavala, B. de Foy, R. Volkamer, L. T. Molina and M. J. Molina, *Atmos. Chem. Phys.*, **7**, 329 (2007).
20. J. M. Etzkorn, N. G. Davey, A. J. Thompson, A. S. Creba, C. W. LeBlanc, C. D. Simpson, E. T. Krogh and C. G. Gill, *J. Chromatogr. Sci.*, **47**, 57 (2009).
21. S. S.-Y. Chui, S. M. F. Lo, J. P. H. Charmant, A. G. Orpen and I. D. Williams, *Science*, **283**, 1148 (1999).
22. K. Okada, R. Ricco, Y. Tokudome, M. J. Styles, A. J. Hill, M. Takahashi and P. Falcaro, *Adv. Funct. Mater.*, **24**, 1969 (2014).
23. Z. Zhao, S. Wang, Y. Yang, X. Li, J. Li and Z. Li, *Chem. Eng. J.*, **259**, 79 (2015).
24. K. M. Choi, J. H. Park and J. K. Kang, *Chem. Mater.*, **27**, 5088 (2015).
25. Y.-R. Lee, J. Kim and W.-S. Ahn, *Korean J. Chem. Eng.*, **30**, 1667 (2013).
26. D. Zacher, O. Shekha, C. Wöll and R. A. Fischer, *Chem. Soc. Rev.*, **38**, 1418 (2009).
27. Y. Hu, J. Liao, D. Wang and G. Li, *Anal. Chem.*, **86**, 3955 (2014).
28. K. Sugikawa, S. Nagata, Y. Furukawa, K. Kokado and K. Sada, *Chem. Mater.*, **25**, 2565 (2013).
29. S. L. Kleinman, R. R. Frontiera, A.-I. Henry, J. A. Dieringer and R. Van Duyne, *Phys. Chem. Chem. Phys.*, **15**, 21 (2013).
30. K. Kim, X. Chong, P. B. Kreider, G. Ma, P. R. Ohodnicki, J. P. Baltrus, A. X. Wang and C. Chang, *J. Mater. Chem. C*, **3**, 2763 (2015).
31. C. D'Andrea, J. Bochterle, A. Toma, C. Huck, F. Neubrech, E. Messina, B. Fazio, O. M. Marago, E. D. Fabrizio, M. L. de la Chapelle, P. G. Gucciardi and A. Pucci, *ACS Nano*, **7**, 3522 (2013).
32. H. Zhang, T. Wang, J. Wang, H. Liu, T. D. Dao, M. Li, G. Liu, X. Meng, K. Chang, L. Shi, T. Nagao and J. Ye, *Adv. Mater.*, **28**, 3703 (2016).
33. K. M. Choi, D. H. Kim, B. Rungtaweevoranit, C. A. Trickett, J. T. D. Barmanbek, A. S. Alshammari, P. Yang and O. M. Yaghi, *J. Am. Chem. Soc.*, **139**, 356 (2017).
34. I.-H. Yoo, S. S. Kalanur, K. Eom, B. Ahn, I. S. Cho, H. K. Yu, H. Jeon and H. Seo, *Korean J. Chem. Eng.*, **34**, 3200 (2017).
35. Y.-T. Yu and P. Mulvaney, *Korean J. Chem. Eng.*, **20**, 1176 (2003).
36. S. Xian, Y. Yu, J. Xiao, Z. Zhang, Q. Xia, H. Wang and Z. Li, *RSC Adv.*, **5**, 1827 (2015).
37. X. Chen, Z. Guo, W. H. Xu, H. B. Yao, M. Q. Li, J. H. Liu, X. J. Huang and S. H. Yu, *Adv. Funct. Mater.*, **21**, 2049 (2011).
38. Z. Q. Tian, B. Ren and D. Y. Wu, *J. Phys. Chem. B*, **106**, 9463 (2002).
39. C. E. Talley, J. B. Jackson, C. Oubre, N. K. Grady, C. W. Hollars, S. M. Lane, T. R. Huser, P. Nordlander and N. J. Halas, *Nano Lett.*, **5**, 1569 (2005).
40. K. Pirzadeh, A. A. Ghoreyshi, M. Rahimnejad and M. Mohammadi, *Korean J. Chem. Eng.*, **35**, 974 (2018).
41. C. Prestipino, L. Regli, J. G. Vitillo, F. Bonino, A. Damin, C. Lamberti, A. Zecchina, P. L. Solari, K. O. Kongshaug and S. Bordiga, *Chem. Mater.*, **18**, 1337 (2006).
42. X. Sun, H. Li, Y. Li, F. Xu, J. Xiao, Q. Xia, Y. Lia and Z. Li, *Chem. Commun.*, **51**, 10835 (2015).

Supporting Information

Surface-enhanced infrared detection of benzene in air using a porous metal-organic-frameworks film

Raekyung Kim*,‡, Seohyeon Jee*,‡, Unjin Ryu*, Hyeon Shin Lee*, Se Yun Kim,†, and Kyung Min Choi*,†**

*Department of Chemical and Biological Engineering, Sookmyung Women's University,
100 Cheongpa-ro 47 gil, Yongsan-gu, Seoul 04310, Korea
**Department of Materials Science & Engineering, KAIST, Daejeon 34141, Korea
(*Received 31 October 2018 • accepted 17 January 2019*)

Method S1: Powder X-ray Diffraction

The crystallinity of each of the nHKUST-1 films was evident from their PXRD diffraction lines. The powder X-ray (PXRD) spectra were obtained by a Rigaku X-ray diffractometer (Smartlab, Cu Kα radiation) at 1,200 W (40 kV, 30 mA). It scanned 4°/min rate from 3° to 50° on a silicon holder.

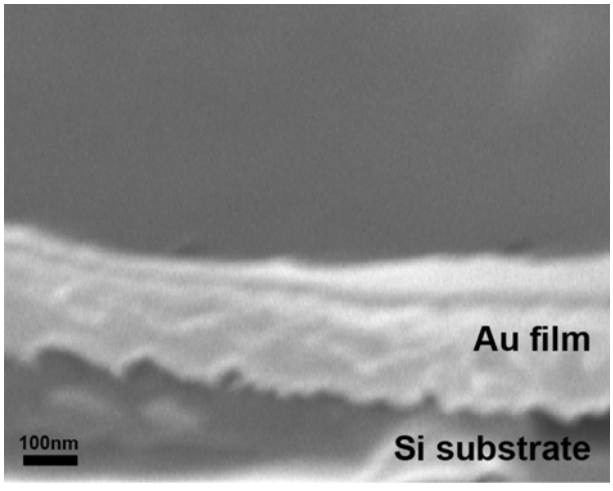

Fig. S1. Planar and cross sectional SEM for Au film deposited on Si substrate.

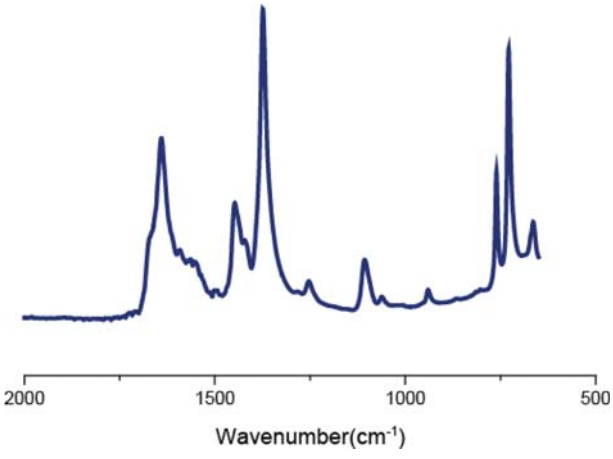

Fig. S2. IR spectra for nanocrystalline HKUST-1.

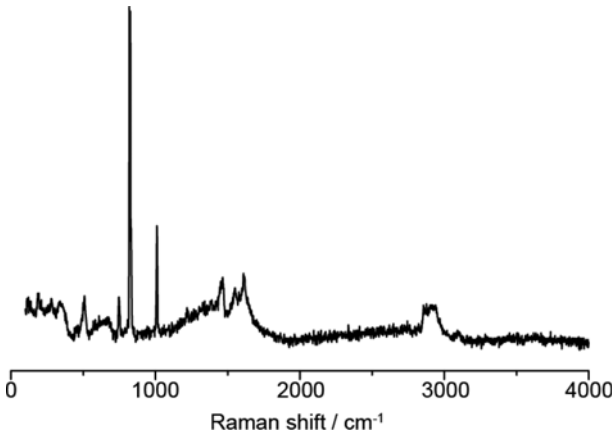

Fig. S3. Raman spectra for nanocrystalline HKUST-1.

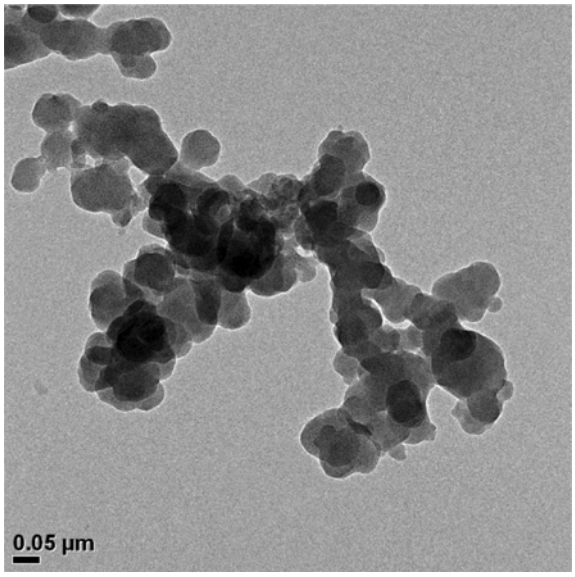

Fig. S4. TEM image for nanocrystalline HKUST-1.

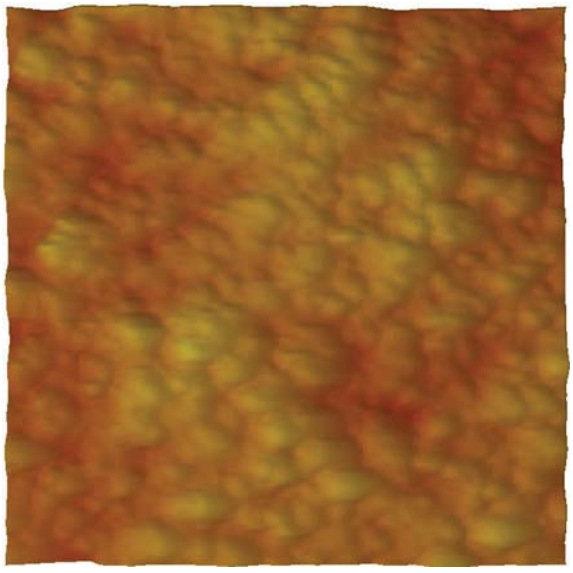

Fig. S5. AFM image for nHKUST-1 film fabricated from 2.4 wt% nHKUST-1 colloidal dispersion.

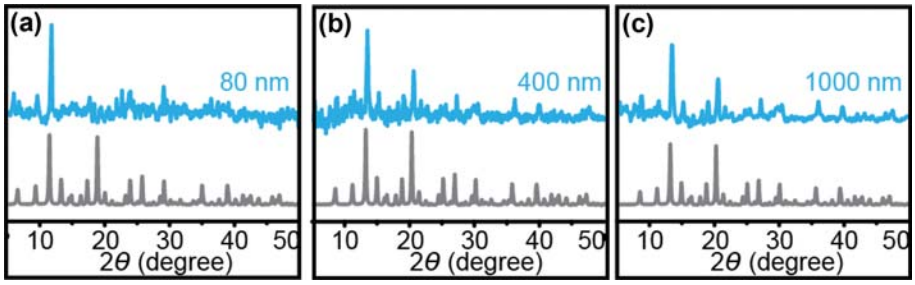

Fig. S6. PXRD patterns of the nHKUST-1 films fabricated using colloidal solutions with different concentrations of nHKUST-1: (a) 1 wt% solution; (b) 2.4 wt% solution; (c) 5 wt% solution.

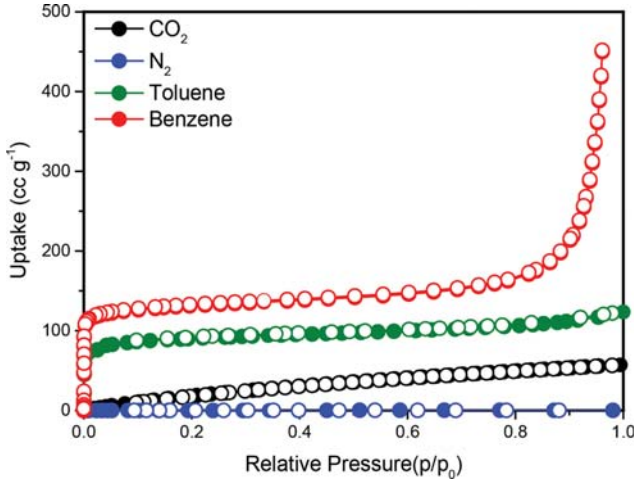

Fig. S7. The sorption isotherm of benzene, nitrogen, carbon dioxide, and toluene in nHKUST-1 at room temperature.

Table S1. Other studies combining MOFs and plasmon enhancement

Ref.	MOFs	Plasmon source	Applications
10	HKUST-1	Ag nanoparticle	CO_2 sensor
27	MIL-101	AuNPs (gold nanoparticle)	Sensing, bioanalytical and biomedical
28	MOF-5	AuNR (gold nanorod)	SERS sensor
30	HKUST-1	Gold nanoantennas	CO_2 sensor
36	MIL-101(Fe)	Fe nanoparticle	Photoinduced CO_2 reduction
37	Re-MOF	Ag nanocube	Photocatalytic CO_2 conversion

Table S2. Other studies for gaseous molecular detection using spectroscopy

Ref.	Materials for molecular capture	Detector	Surface enhancement effect	Plasmon source	Sensor fabrication method	Target molecules or (gas)	Target molecule sorption range
10	HKUST-1	Localized surface plasmon resonance (LSPR)	Yes	Ag	Layer-by-layer method	SF^6	$\sim10^{-4}$ refractive index units (RIU)
11	Au-CeO_2	LSPR gag sensor (UV-NIR)	Yes	Au	Molecular beam epitaxy	H_2, CO, NO_2	100-10,000 ppm 200-2,000 ppm 2-98 ppm
12	Au-NiO Au-TiO_2(Pt)	LSPR gag sensor (UV-NIR)	Yes	Au	Sol-gel method	H_2, CO	~1%
13	TiO_2-Au	UV, LSPR gag sensor (UV-NIR)	Yes	Au	Spin coating, dropa casting, ink-jet printing	CO, H_2, Ethanol	10 ppm~1%
14	Au-nanorod	UV, LSPR gag sensor (UV-NIR)	Yes	Au	Solvthermal, dispersed	H_2, CO, NO_2	100 ppm~1%
15	Ag@Co_3O_4	TGA	Yes	Ag	Drop and coated	HCOH, Ethanol, Acetone, Methylbenzene	10-100 ppm
16	Ag@SnO_2	UV-vis	Yes	Ag	Patterning	CO	~200 ppm
18	Activated carbon	IR	No	No	Tunable diode laser absorption spectroscopy (TDLAS) instrumentation	Benzene	100 ppm~2%
20	membrane	Membrane introduction mass spectrometry (MIMS)	No	No	Membrane	VOCs	ppbv
36	MIL-101(Cr)	Intelligent gravimetric analyzer (IGA)	No	No	-	VOCs	N/A
37	Ag@SnO, Ag/SnO_{22}	UV-vis	No	Ag	Sol-gel method	Ethanol	20-250 ppm